Journal of Thermal Analysis and Calorimetry (2024) 149:5257–5264
https://doi.org/10.1007/s10973-024-13204-6

Monitoring of some minor human skin lesions using a skin calorimeter

Pedro Jesús Rodríguez de Rivera[1] · Miriam Rodríguez de Rivera[2] · Fabiola Socorro[1] · Manuel Rodríguez de Rivera[1]

Received: 21 July 2023 / Accepted: 8 April 2024 / Published online: 2 May 2024

Abstract

The growing interest of human skin thermal properties is motivating the development of new instruments, either by contact or by remote sensing. In this work, we show the ability of a skin calorimeter to monitor the temporal evolution of the heat capacity and the equivalent thermal resistance of the skin, in two small skin lesions. The first one consists of a forehead wound of 10×2 mm^2. The other injury consists of a second degree burn on the volar wrist area, of 10×20 mm^2. We studied the temporal evolution of the thermal properties of both injuries. The variation of heat capacity was significant. For first injury, heat capacity decreased by 21% and full recovery was achieved after ten days. For the second case, the heat capacity decrease was 55% and recovery was achieved after 3 weeks. These skin recoveries are monitored by the measured heat capacity value. The returning of the heat capacity to its normal value coincides with the recovery from the injury.

Keywords Direct calorimetry · Non-differential calorimetry · Skin thermal properties · Skin injury

Abbreviations

C	Heat capacity, JK^{-1}
C_1, C_2	Of the calorimetric model domains
C_{skin}	Of the skin under the calorimeter
C_0	Measurement offset
P	Thermal conductance, WK^{-1}
P_1, P_2, P_{12}	Of the calorimetric model
P_{skin}	Of the skin under the calorimeter
$y(t)$	Calorimetric signal, V
k	Measurement thermopile Seebeck coefficient, VK^{-1}
ε_y	Calorimetric signal root mean square error, V
T	Temperature, °C
$T_1(t)$, $T_2(t)$	Of the calorimetric model domain
T_{cold}	Of the cold focus
T_{room}	Of ambient
W	Power, W
$W_1(t)$, $W_2(t)$	Of the calorimetric model domain
$W_{skin}(t)$	Of the skin
R_{skin}	Thermal resistance of the skin, KW^{-1}
t, t_{max}	Time, final time, s
$\Delta\tau$	Sampling period, s

✉ Manuel Rodríguez de Rivera
manuel.rguezderivera@ulpgc.es

[1] Department of Physics, University of Las Palmas de Gran Canaria, Las Palmas de Gran Canaria, Spain

[2] Cardiology Service, Hospital Universitario Marqués de Valdecilla, Santander, Spain

Introduction

In medical instrumentation, thermometry has a common use among all medical specialties. However, there is no standard application of the measurement of the heat flux dissipated by the human body, except in two fields of current interest. In the first one, heat flux measurements are used to evaluate room thermal conditions in accordance with the capacity and the use of the space. In the second application, these measurements are used to determine the metabolic activity of human body. Two techniques are commonly used to measure heat flux: direct calorimetry and indirect calorimetry [1, 2].

Currently, the main technique used to express the energy consumption of a physical activity is the indirect calorimetry, which is based on the measurement of the VO_{2max} consumed by a subject [3]. This energy is expressed in multiples of the resting metabolic rate (RMR), with the metabolic equivalent (MET) being the unit used (1 MET corresponds with the consumption of 3.5 mL kg^{-1} min^{-1} of O_2). This parameter varies from 1 MET at rest to 3–6 METs at moderate physical activity. More than 6 METs correspond to an intense physical activity.

On the other hand, it is also interesting the measurement of the heat loss of specific areas of the human body. Several

authors have made localized heat flux measurements to study heat dissipation at rest, as a function of clothing level, in response to heating and cooling, exercise, or extreme weather conditions. These measurements have been performed mainly with heat flow sensors [4–6].

Instruments and techniques have also been developed to characterize the thermal properties of the skin [7–12], that change in response to alterations or pathologies [8]. The principle of operation of these devices consists of analyzing the static and dynamic response to a thermal excitation produced by the device itself. Depending on the heat transfer phenomena that describe the energy exchange, the model required to relate the measured values with the skin properties may vary. We developed a skin calorimeter able to measure the heat flow, the thermal resistance and the heat capacity of a 4 cm^2 skin surface. The measurement procedure consists of applying the calorimeter on the skin, in a way in which the heat transfer between the skin and the calorimeter thermostat is mainly by conduction [13]. In this paper we show the ability of this skin calorimeter to monitor the heat capacity and the thermal resistance of two small skin lesions. First, we briefly describe the experimental system and establish a measurement procedure. Then, we relate the heat capacity of the model with the skin heat capacity, and finally we show the results and the conclusions of this work.

Materials and methods

Experimental

In previous work [13], the device used has been described in detail. This calorimeter consists basically of a thermostated thermopile. The device is designed to produce controlled thermal excitations on a 4 cm^2 skin region, by varying its thermostat temperature. Thus, a fast cooling system is required. For this purpose, we use a Peltier element. The skin response will depend on its actual (in vivo) thermal properties. A schematic of the device is shown in Fig. 1. Calibration is performed in two ways. Firstly, by placing the calorimeter on an EPS calibration base able to perform Joule calibrations. On the other hand, inert substances with known thermal properties are also used. To operate the calorimeter, a power supply, a data acquisition system and a control and measurement program are required. This program is written in C++ and controls the instrumentation with a sampling period of 0.5 s.

Calibration

To represent the heat transfer phenomena between the skin and the calorimeter, we use a two-body model [14, 15]. The first body represents the substances affected by the skin

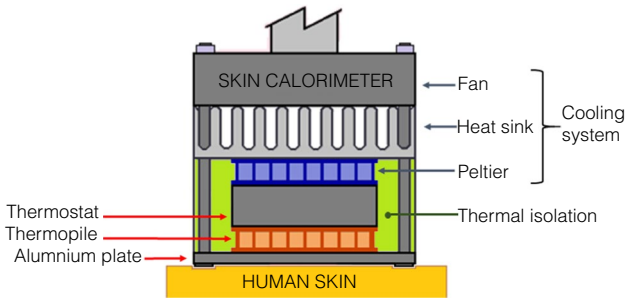

Fig. 1 Schematic of the skin calorimeter ($2\times2\times2$ cm^3)

thermal behavior and the second one correspond to the calorimeter's thermostat. Each body develops a power (W_1, W_2), has a temperature (T_1, T_2), a heat capacity (C_1, C_2) and is joined by thermal couplings with the other body (P_{12}) and with the ambient (P_1, P_2). Considering constant the ambient temperature (T_{room}) and the cooling thermopile supply (T_{cold}), we can correct the baselines to their initial steady state, obtaining the system:

$$\begin{aligned}\Delta W_1(t) &= \frac{C_1}{k}\Delta y'(t) + \frac{P_1+P_{12}}{k}\Delta y(t) + C_1\Delta T_2'(t) + P_1\Delta T_2(t)\\ \Delta W_2(t) &= -\frac{P_{12}}{k}\Delta y(t) + C_2\Delta T_2'(t) + (P_{12}+P_2)\Delta T_2(t)\end{aligned} \tag{1}$$

where $y(t)$ is the signal provided by the measurement thermopile, whose Seebeck coefficient is k.

The calorimeter calibration consists of identifying this model, i.e., determining the coefficients of Eq. 1 (C_1, C_2, P_1, P_2, P_{12}, k). For this purpose, is required a specific calibration measurement where powers W_1 (calibration power) & W_2 (thermostat power) are controlled, and the calorimetric signal (y) and thermostat temperature (T_2) are measured. Using an iterative process based on the Nelder-Mean algorithm [16, 17] we can identify the parameters of the model with an acceptable error. Figure 2 shows the signals of a calibration measurement.

Skin thermal properties determination

Note that all parameters are constant except C_1 and P_1, that depend on the substance under the calorimeter. To determine C_1 and P_1 in the case of applying the device on the human skin, we use the first equation of the system of equations Eq. 1. This equation (Eq. 2) relates the calorimeter's temperature (ΔT_2) and the calorimetric signal (Δy) with the skin heat flow (ΔW_{skin}).

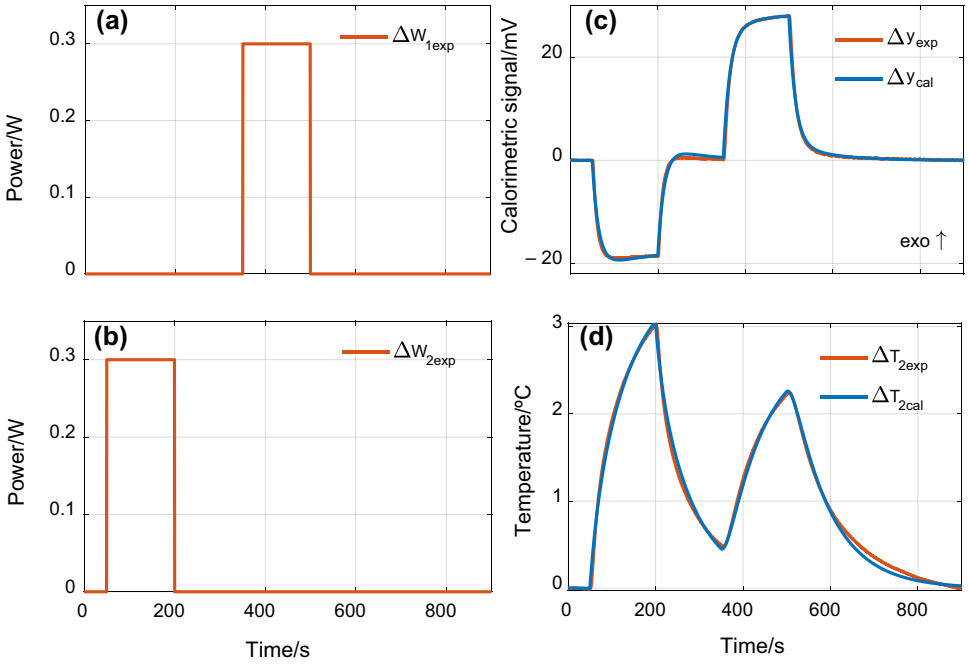

Fig. 2 Calibration measurement. Power dissipated at the calibration base (**a**) and at the thermostat (**b**). Calorimetric output (**c**) and thermostat temperature (**d**). Experimental (red) and model-calculated (blue) output curves are shown

$$\Delta W_{\text{skin}}(t) = \frac{C_0 + C_{\text{skin}}}{k}\Delta y'(t) + \frac{P_{\text{skin}} + P_{12}}{k}\Delta y(t) + (C_0 + C_{\text{skin}})\Delta T_2'(t) + P_{\text{skin}}\Delta T_2(t) \quad (2)$$

Now, $C_0 + C_{\text{skin}}$ replaces C_1, and P_{skin} replaces P_1. The C_0 heat capacity is the calorimeter offset ($C_0 = 2.81$ JK^{-1}), previously determined [13], by measurements of known heat capacity samples (Teflon, brass & aluminum).

The measurement consists of applying the sensor on the skin and produce a thermal excitation. This excitation consists of a variation of the calorimeter thermostat temperature between two steady states (Fig. 3b). This temperature change produces a thermostat power (Fig. 3c) and a calorimetric

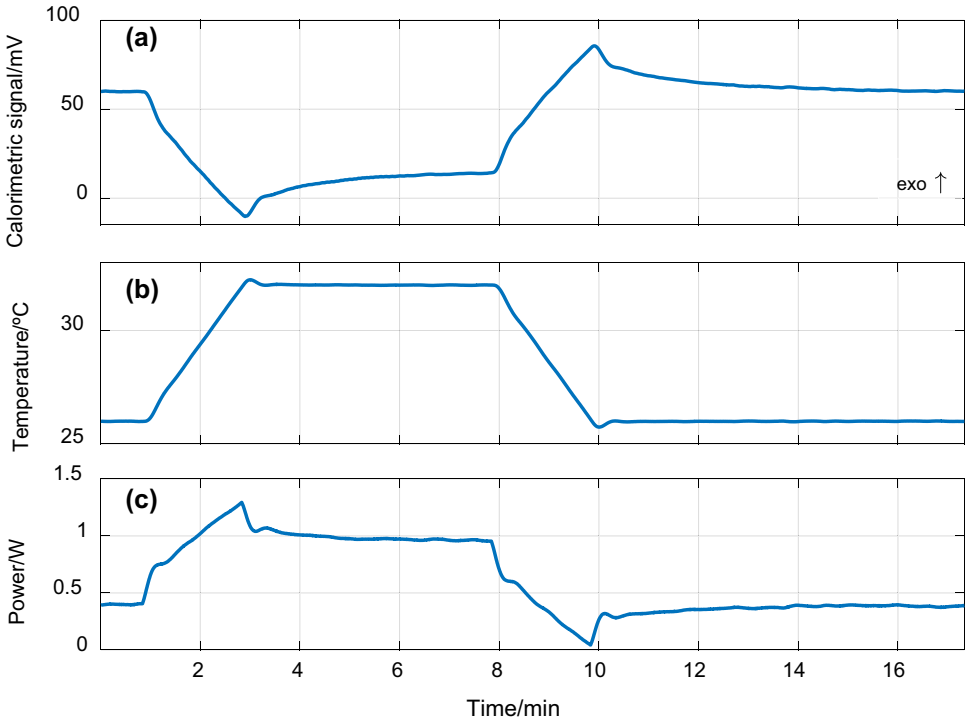

Fig. 3 Measurement for skin thermal properties determination. **a** Calorimetric signal (y). **b** calorimeter temperature (T_2). and **c** calorimeter power (W_2)

signal (Fig. 3a) response, that depends on the speed and the stabilization time after the linear temperature change (3 °C min^{-1} & 5 min in the case shown). Heating and cooling of the thermostat have been programmed, so we obtain two different results.

The process of identifying the thermal properties of the skin is an iterative algorithm similar to that used in calibration. In order to obtain a consistent result, it is necessary to understand the behavior of the skin, which can greatly simplify the calculation process. From previous works [18], we consider two hypotheses:

1. We consider that $\Delta W_{skin}(t)$ has the opposite and inverse shape of the calorimeter temperature $\Delta T_2(t)$.
2. P_{skin} is the quotient between the changes of calorimeter temperature and heat flux: $\Delta T_2(t_{max})/\Delta W_{skin}(t_{max})$, being P_{12} the offset the thermal conductance measurement and t_{max} the time of signals stabilization.

As an example, this procedure has been applied to the measurement shown in Fig. 3, performed on the central forehead area of a healthy male subject of 64 years. Heat capacity and heat flux variation has been determined. Figure 4 shows the calorimetric signal fit (between experimental and calculated curves) and the root mean square error ε_y for the 900 experimental points ($\Delta t = 0.5$ s). The calculation has been performed for both the heating and cooling zones, and the results are slightly different. As mean value, we have $C_{skin} = 2.055 \pm 0.045$ J K^{-1}, $\Delta W_{skin}(t_{max}) = 140.5 \pm 4.5$ mW and $R_{skin} = 33.6 \pm 1.4$ K W^{-1}. This result gives the uncertainty in the determination of the heat capacity, heat flux variation and thermal resistance of the 4 cm^2 skin region under the calorimeter. This is the sensor's own uncertainty. However, this uncertainty seems to increase when measurements are made on different days, on the same subject, and under the same conditions. This is caused by the inherent variability of the human body. To evaluate this variability, the heat capacity and the thermal resistance of seven different abdominal areas, separated from each other by 10 cm, were measured daily for one month. These measurements were performed on the same subject analyzed in this paper, at the same resting conditions. The results reveal a heat capacity of $C_1 = 4.5 \pm 0.2$ J K^{-1} and a thermal resistance of $R_1 = 36.4 \pm 1.8$ K/W. In all these measurements blood pressure (BP) and heart rate (HR) were determined with an automatic BP monitor (systolic BP 113 ± 5 mmHg, diastolic BP 82 ± 2 mmHg, and HR 81 ± 6 bpm). Room temperature was 22.5 ± 0.8 °C and relative humidity $59 \pm 2\%$. There was no condensation on the skin or the sensor in any measurement of this work. In addition, the subject was at rest and not sweating. To check the possible variation of skin moisture, this parameter was measured by electrical bioimpedance with two electrodes separated by 7 mm (Agatige Skin Moisture Meter Digital), obtaining values of $22.8 \pm 2.3\%$. Perhaps

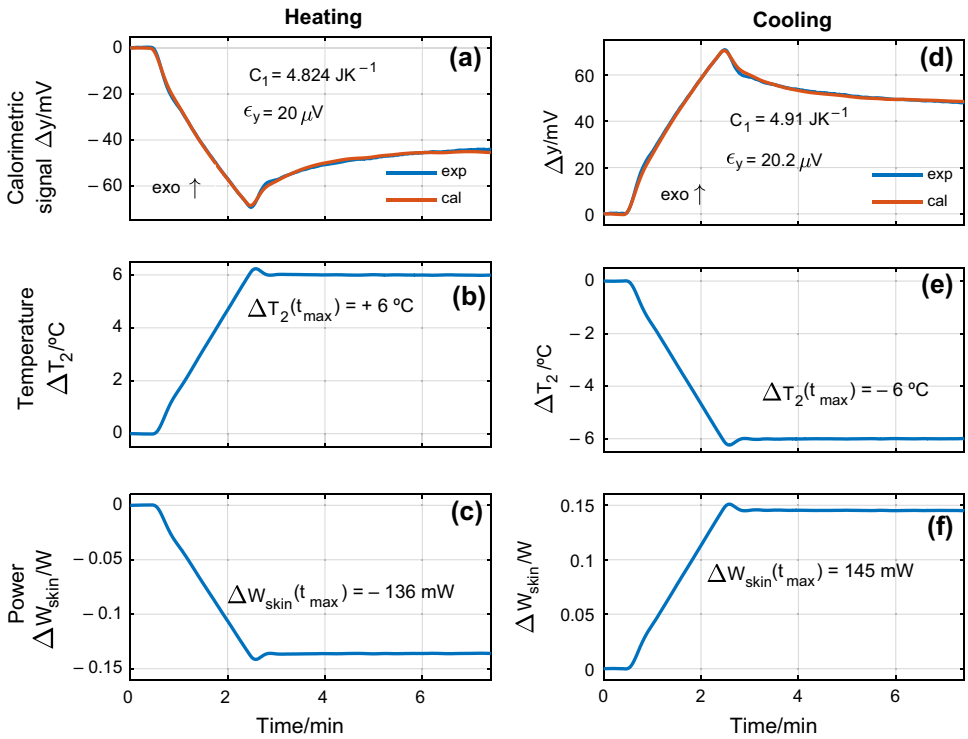

Fig. 4 Determination of the heat capacity from the measurement shown in Fig. 3 for heating (**a**, **b**, **c**) and cooling (**d**, **e**, **f**) sections. Adjustment of the calorimetric signal (**a**, **d**), thermostat temperature variation (**b**, **e**) and heat flux variation (**c**, **f**) (experimental curves in blue, calculated curves in red)

vasoconstriction or vasodilatation could play a role in these results, although is not demonstrated in this work. These data will help to understand the results below, especially to discern when the changes are significant.

Results and discussion

Evolution of a small forehead injury

Now, we will apply the measurement procedure explained on two small skin lesions. Measurements were performed daily on the injured area. The first injury studied is a 10 mm long & 2 mm wide forehead wound. This injury was caused by a domestic accident, in which the subject was struck by the edge of a wooden door. Figure 5 shows the injury on days 1, 3 and 9. It is also shown the calorimeter placement with an adapted clamp. On day 1, rapid healing and slight inflammation is observed. On day 3 there is no apparent inflammation, and on day 9 the skin is almost healed.

From the first day, measurements were performed with the skin calorimeter. The measurement procedure for each day was identical, in this case the temperature jump of the thermostat was 6 °C (with a 3 °C min^{-1} speed) and a stabilization time of 5 min. These type of measurement is similar to the shown in Fig. 3. It is important to note that all measurements are identical, so the thermal penetration is considered to be the same. As consequence, the results are comparable. During the measurements, the subject was seated and at rest. The subject is a healthy male of 64 years old. Ambient room temperature on the 18 days measured was 17.5 ± 0.4 °C.

Fig. 5 Evolution of the small forehead wound: **a** day 1, **b** day 3, **c** day 9, **d** skin calorimeter on the skin

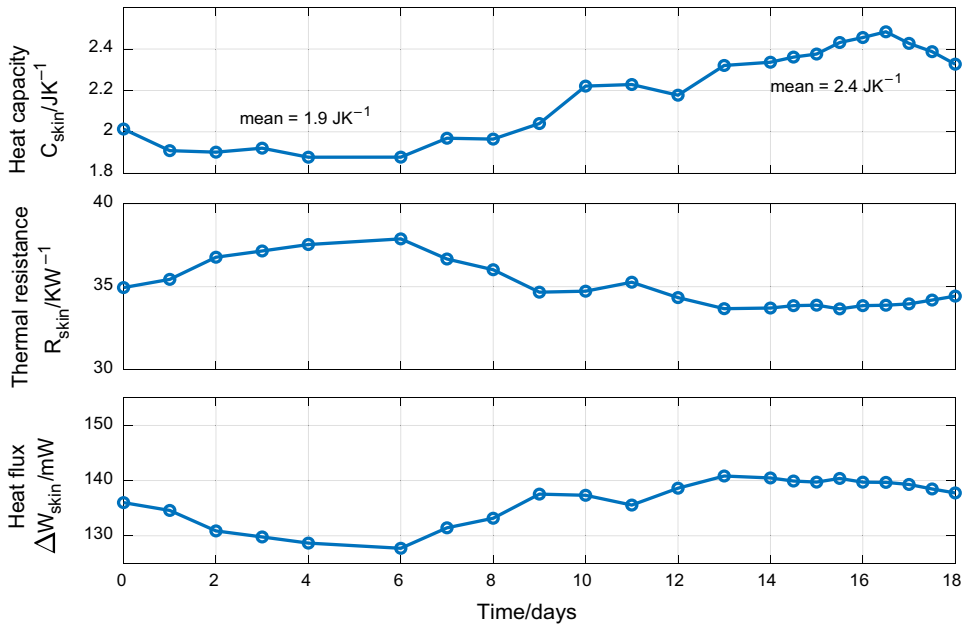

Fig. 6 Evolution of heat capacity, thermal resistance and heat flux variation for a minor forehead wound (Fig. 5)

Fig. 7 Evolution of the burn on the volar zone of the right wrist: **a** day 1, **b** day 7, **c** day 14, **d** day 27

Figure 6 shows the results obtained for heat capacity, equivalent thermal resistance and heat flux variation. Heat capacity decreased by 21% of the final value (when the lesion is already recovered). However, the initial heat flux is 10% lower than the final value and, as a consequence, there is an equivalent change of the thermal resistance value. We consider that the variation in heat flux is not significant enough to be taken into account in the assessment of this lesion. The heat flux depends on the overall physical state of the subject, even if the measurement is local. For the following injury, a differential configuration study will be performed.

Evolution of a small second degree burn: differential study

The second injury studied was a second-degree burn to the volar area of the right wrist. This injury occurred in a domestic accident with an iron. The lesion has an area of approximately 2×1 cm^2. Figure 7 shows the temporal evolution of the injury on days 1, 7, 14 and 27. On the first day, the formation of a fluid blister is observed. On the seventh day, the injury is in the process of healing, on the eighth day 70% of the injury is almost healed and on the 27th day the recovery is almost consolidated. During the measurements, the subject was seated and at rest. The subject is a healthy male of 64 years old. Ambient room temperature on the 35 days measured was 23.0 ± 1 °C and a relative humidity of 58 ± 2%.

In this case, a differential study was performed. The measurements were taken in the volar areas of the right (injured) and left (healthy) wrists. On the other hand, in order to have a higher signal/noise ratio, the temperature jump used was 10 °C and the heating speed was 4 °C min^{-1}. As in the previous case, to ensure equal thermal penetration in all measurements, the thermostat temperature setting for all measurements was the same, with a stabilization time of 5 min. Figure 8 shows the results. The curves on the left show the results obtained for each case (injured and healthy). The curves on the right show the result in differential. It is important to note that the thermal resistance is directly related with the variation of the measured area heat flux for a given temperature change. This heat flux is highly variable, since it depends on the overall condition of the subject and his physical activity.

Although these measurements were performed while the subject was seated and resting, the differential measurement can give a more specific result of the injury. We observe that in the differential result, the heat capacity of the injured area is 1.33 J K^{-1} lower than the final mean value, 2.4 J K^{-1}, i.e. 55%. However, the variation of the differential heat flux has an oscillation of ± 5 mW, of the same order of magnitude as the resolution of the experimental system. It is true that there are muscular lesions in which heat flow increases in comparison with areas close to the lesion, that can be monitored with infrared thermography [19]. But this is not our case.

To summarize, the injury has produced a clear decrease in the calorific capacity and its recovery can be quantified day by day by the evolution of the measured heat capacity. In this case, on day 20 heat capacity reaches its normal value, meaning the recovery from the injury.

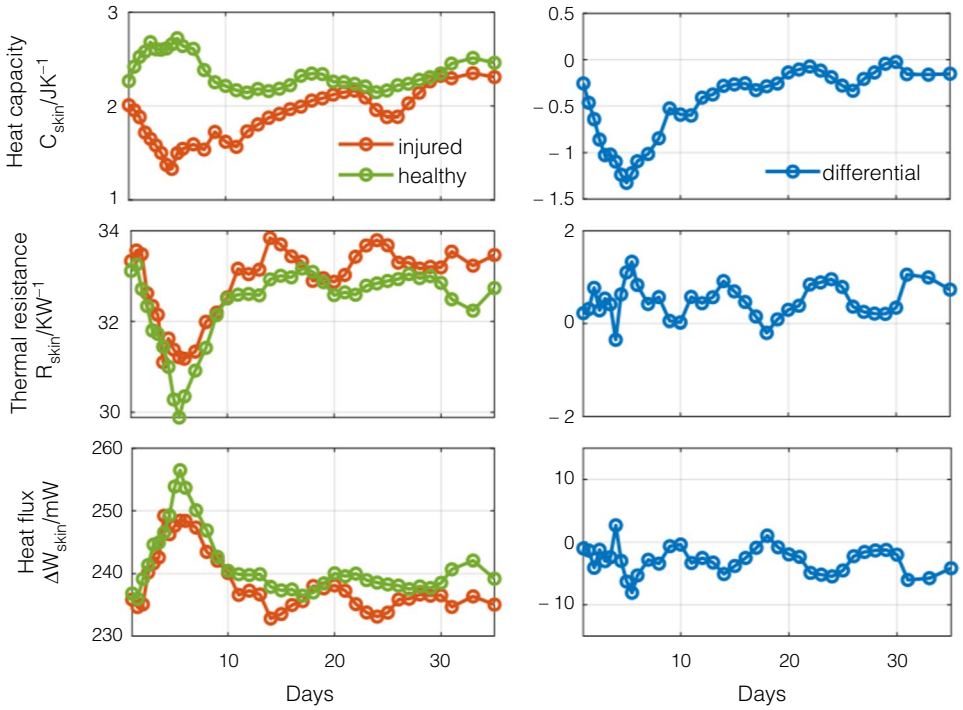

Fig. 8 Variation of heat capacity and equivalent thermal resistance in a second-degree burn on the volar wrist area of a healthy 62-year-old male subject

Conclusions

1. We have developed a methodology to monitor the thermal resistance and the heat capacity of a localized region of the skin.
2. In the small lesions monitored, we observed a clear dependence of the injury recovery on the measured heat capacity value.
3. Thermal resistance depends directly on heat flux, and since heat flux depends on the overall physical state of the subject, differential measurements have advantages over non-differential measurements for the case study of some particular injuries.
4. The skin calorimeter is a novel technique that requires many measurements to prove its usefulness in clinical practice. Although the prototype is somewhat bulky, its effectiveness is clear, and this study is useful for the future construction of similar, more integrated devices that could form part of the so-called "wearable devices".

Author contributions Conceptualization, P.R. and M.R.; methodology, P.R.; software, M.R.; validation, F.S., Mi.R. and P.R.; formal analysis, M.R.; investigation, P.R.; resources, F.S.; data curation, Mi.R.; writing—original draft preparation, M.R.; writing—review and editing, M.R.; visualization, P.R.; supervision, F.S.; project administration, Mi.R. All authors have read and agreed to the published version of the manuscript.

Funding Open Access funding provided thanks to the CRUE-CSIC agreement with Springer Nature. This research received no external funding.

Declarations

Conflict of interest The authors declare no conflict of interest.

References

1. Jacobsen S, Johansen O, Garby L. A 24–m^3 direct heat-sink calorimeter with on-line data acquisition, processing, and control. Am J Physiol. 1985. https://doi.org/10.1152/ajpendo.1985.249.4.E416.
2. Kenny GP, Notley SR, Gagnon D. Direct calorimetry: a brief historical review of its use in the study of human metabolism and thermoregulation. Eur J Appl Physiol. 2017. https://doi.org/10.1007/s00421-017-3670-5.
3. Sjödin AM, Forslund AH, Westerterp KH, Andersson AB, Forslund JM, Hambræus LM. The influence of physical activity on

BMR. Med Sci Sports Exerc. 1996. https://doi.org/10.1097/00005768-199601000-00018.
4. Xu X, Karis AJ, Buller MJ, Santee WR. Relationship between core temperature, skin temperature, and heat flux during exercise in heat. Eur J Appl Physiol. 2013. https://doi.org/10.1007/s00421-013-2674-z.
5. Eggenberger P, MacRae BA, Kemp S, Bürgisser M, Rossi RM, Annaheim S. Prediction of core body temperature based on skin temperature, heat flux, and heart rate under different exercise and clothing conditions in the heat. Front Physiol. 2018. https://doi.org/10.3389/fphys.2018.01780.
6. Jung W, Jazizadeh F, Diller TE. Heat flux sensing for machine-learning-based personal thermal comfort modeling. Sensors. 2019. https://doi.org/10.3390/s19173691.
7. Okabe T, Fujimura T, Okajima J, Aiba S, Maruyama S. Non-invasive measurement of effective thermal conductivity of human skin with a guard-heated thermistor probe. Int J Heat Mass Transfer. 2018. https://doi.org/10.1016/j.ijheatmasstransfer.2018.06.039.
8. Okabe T, Fujimura T, Okajima J, Kambayashi Y, Aiba S, Maruyama S. First-in-human clinical study of novel technique to diagnose malignant melanoma via thermal conductivity measurements. Sci Rep. 2019. https://doi.org/10.1038/s41598-019-40444-6.
9. Webb RC, Pielak RM, Bastien P, et al. Thermal transport characteristics of human skin measured in vivo using ultrathin conformal arrays of thermal sensors and actuators. PLoS ONE. 2015. https://doi.org/10.1371/journal.pone.0118131.
10. Madhvapathy SR, Patel M, Krishnan S, Wei C, Li Y, Xu S, Feng X, Huang Y, Rogers JA. Epidermal electronic systems for measuring the thermal properties of human skin at depths of up to several millimeters. Adv Funct Mater. 2018. https://doi.org/10.1002/adfm.201802083.
11. Zubiaga A, Kirsch C, Boiger G, Bonmarin M. A simple instrument to measure the thermal transport properties of the human skin. In: 2021 IEEE International Symposium on Medical Measurements and Applications (MeMeA). 2021; https://doi.org/10.1109/MeMeA52024.2021.9478754
12. Zhang X, Bontozoglou C, Xiao P. In vivo skin characterizations by using opto-thermal depth-resolved detection spectra. Cosmetics. 2019. https://doi.org/10.3390/cosmetics6030054.
13. Rodríguezde Rivera PJ, Rodríguezde Rivera MI, Socorro F, Rodríguezde Rivera M. Validation of a skin calorimeter to determine the heat capacity and the thermal resistance of the skin. Sensors. 2023. https://doi.org/10.3390/s23094391.
14. Torra V, Tachoire H. Conduction calorimeters heat transmission systems with uncertainties. J Therm Anal Calorim. 1998. https://doi.org/10.1023/A:1010181617076.
15. Socorro F, Rodríguezde Rivera M, Jesús C. A thermal model of a flow calorimeter. J Therm Anal Calorimet. 2001. https://doi.org/10.1023/A:1011582306796.
16. Nelder JA, Mead C. A simplex method for function minimization. Comput J. 1965. https://doi.org/10.1093/comjnl/7.4.308.
17. Lagarias JC, Reeds A, Wright MH, Wright PE. Convergence properties of the nelder-mead simplex method in low dimensions. SIAM J Optim. 1998. https://doi.org/10.1137/S1052623496303470.
18. Rodríguez de Rivera PJ, Rodríguez de Rivera MI, Socorro F, Rodríguez de Rivera M. Measurement of human body surface heat flux using a calorimetric sensor. J Therm Biol. 2019. https://doi.org/10.1016/j.jtherbio.2019.02.022.
19. Dos Santos Bunn P, Koppke M, Rodrigues AI, de Souza Sodré R, Borba Neves E, Bezerra da Silva E. Infrared thermography and musculoskeletal injuries: a systematic review with meta-analysis. Infrared Phys Technol. 2020. https://doi.org/10.1016/j.infrared.2020.103435.